

Q-DPTS: Quantum Differentially Private Time Series Forecasting via Variational Quantum Circuits

Chi-Sheng Chen
Independent Researcher
 Cambridge, USA
 m50816m50816@gmail.com

Samuel Yen-Chi Chen
Wells Fargo
 New York, USA
 yen-chi.chen@wellsfargo.com

Abstract—Time series forecasting is vital in domains where data sensitivity is paramount, such as finance and energy systems. While Differential Privacy (DP) provides theoretical guarantees to protect individual data contributions, its integration especially via DP-SGD often impairs model performance due to injected noise. In this paper, we propose Q-DPTS, a hybrid quantum-classical framework for Quantum Differentially Private Time Series Forecasting. Q-DPTS combines Variational Quantum Circuits (VQCs) with per-sample gradient clipping and Gaussian noise injection, ensuring rigorous (ϵ, δ) -differential privacy. The expressiveness of quantum models enables improved robustness against the utility loss induced by DP mechanisms. We evaluate Q-DPTS on the ETT (Electricity Transformer Temperature) dataset, a standard benchmark for long-term time series forecasting. Our approach is compared against both classical and quantum baselines, including LSTM, QASA, QRWKV, and QLSTM. Results demonstrate that Q-DPTS consistently achieves lower prediction error under the same privacy budget, indicating a favorable privacy-utility trade-off. This work presents one of the first explorations into quantum-enhanced differentially private forecasting, offering promising directions for secure and accurate time series modeling in privacy-critical scenarios.

Index Terms—Quantum machine learning, Differential privacy, Time series forecasting, Variational quantum circuits, ETT dataset.

I. INTRODUCTION

The rapid growth of data-driven applications in health-care, finance, and smart infrastructure has highlighted the dual need for powerful predictive models and rigorous privacy guarantees. Time series data, in particular, often contain sensitive personal or organizational information, making the integration of privacy-preserving mechanisms into forecasting algorithms a pressing concern.

Differential Privacy (DP) has emerged as a principled approach to ensure individual-level data protection by injecting controlled noise into the learning process [1]. In parallel, Quantum Machine Learning (QML) has garnered

The views expressed in this article are those of the authors and do not represent the views of Wells Fargo. This article is for informational purposes only. Nothing contained in this article should be construed as investment advice. Wells Fargo makes no express or implied warranties and expressly disclaims all legal, tax, and accounting implications related to this article.

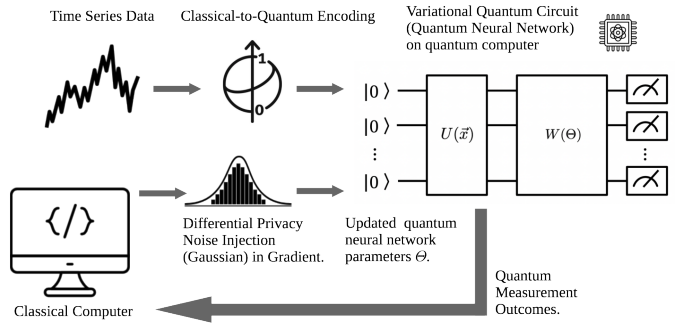


Fig. 1. The overview of this work.

attention for its potential to outperform classical models in specific learning regimes due to richer representational capacity and quantum-enhanced optimization [2]. However, despite their respective advances, the intersection of time-series data on quantum models and differential privacy remains largely unexplored, particularly in the domain of temporal data modeling.

In this work, we present **Q-DPTS**, as shown in Fig. 1, the first quantum forecasting framework that satisfies differential privacy. Q-DPTS leverages variational quantum circuits (VQCs) as core computational modules for time series modeling, while applying Rényi Differential Privacy (RDP) accounting [3] and Gaussian mechanism-based gradient perturbation during training. This hybrid approach combines the generalization capabilities of quantum models with provable privacy guarantees.

We implement and evaluate four quantum architectures: Quantum Long Short-Term Memory (QLSTM) [4], Quantum Recurrent Weighted Key-Value (QRWKV) [5], and Quantum Adaptive Self-Attention (QASA) [6]. Each model is trained under varying noise multipliers corresponding to different privacy budgets ($\sigma = 0, 0.5, 1.0, 2.0$), and is assessed using mean absolute error (MAE), mean squared error (MSE), and root mean squared error (RMSE) on the ETT dataset [7], a benchmark for multivariate time series forecasting.

To the best of our knowledge, this is the first work to

explore differentially private training of variational quantum models for time series forecasting. Our contributions are threefold:

- We propose Q-DPTS, the first framework to integrate differential privacy into quantum forecasting models.
- We design and implement a suite of hybrid quantum-classical architectures compatible with DP-SGD training using RDP-based noise accounting.
- We benchmark model performance under various privacy levels, revealing that certain quantum models (notably QASA and QLSTM) demonstrate robustness to noise and maintain competitive forecasting accuracy.

Our findings suggest that differentially private quantum forecasting is not only feasible but also effective, offering a promising direction for privacy-preserving modeling in quantum-enhanced environments.

II. RELATED WORKS

A. Quantum Time Series Forecasting

Quantum machine learning (QML) [8] has recently been applied to time series modeling, aiming to leverage the high expressivity and entanglement properties of parameterized quantum circuits (PQCs). Hybrid quantum-classical models such as Quantum Long Short-Term Memory (QLSTM) and variational quantum circuits (VQCs) have demonstrated the ability to capture complex temporal dependencies [9]. Other architectures, including quantum-enhanced attention mechanisms and Fourier-based encoders, have also been proposed for forecasting and anomaly detection in sequential datasets [10]. However, existing quantum models are typically evaluated under idealized noise-free settings and assume full access to raw training data, which limits their real-world applicability in privacy-sensitive domains.

B. Differential Privacy in Time Series Forecasting

Differential privacy (DP) has been widely adopted as a formal mechanism to protect individual data points in machine learning workflows. In time series forecasting, DP-SGD [11] and Rényi Differential Privacy (RDP) accounting have been successfully integrated into deep learning models to limit the privacy leakage of sensitive sequences. Recent efforts have explored differentially private recurrent networks [12], federated time series prediction [13], and privacy-preserving sensor modeling. However, these techniques have only been applied to classical architectures, and their extension to quantum models has not yet been realized.

C. Quantum Differential Privacy

The intersection of quantum computing and differential privacy remains largely theoretical. Early work in quantum cryptography has explored the definition of quantum differential privacy (QDP) in the context of quantum data

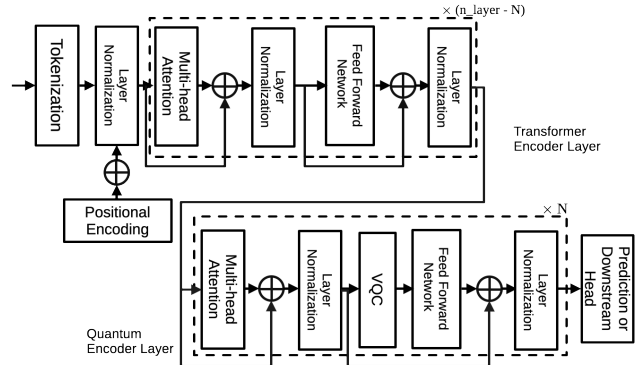


Fig. 2. The model architecture of QASA.

and queries [14]. More recent studies have proposed privacy guarantees for quantum algorithms via measurement noise or randomized response techniques [15]. Nonetheless, no existing research has implemented DP-SGD within variational quantum learning pipelines for practical machine learning tasks such as forecasting. Our work fills this gap by being the first to empirically evaluate the effect of DP-induced noise on quantum forecasting models and to benchmark multiple quantum architectures under different privacy budgets.

III. METHODOLOGY

We present four quantum time series forecasting models built on hybrid quantum-classical architectures. Each model encodes a fixed-length historical window of $T = 16$ time steps of multivariate data $\mathbf{X} = [\mathbf{x}_{t-T+1}, \dots, \mathbf{x}_t] \in \mathbb{R}^{T \times d}$ into a quantum representation, processes it with variational quantum circuits (VQCs), and predicts the value \hat{y}_{t+1} of the next time step. This setting follows a 16-step input \rightarrow 1-step output formulation, distinct from sequence-to-sequence models.

All models support differentially private training using DP-SGD. At each training step, gradients are clipped to a fixed ℓ_2 norm bound C , and Gaussian noise $\mathcal{N}(0, \sigma^2 C^2)$ is added before averaging and updating the parameters. Privacy guarantees are tracked using Rényi Differential Privacy (RDP) accounting, where the total privacy loss ϵ is computed as a function of noise multiplier σ , number of steps T , sampling rate β , and target δ :

$$\epsilon(\sigma, T, \beta, \delta) \leq \min_{\alpha > 1} \left(\frac{1}{\alpha - 1} \log \left(\frac{1}{\delta} \right) + \frac{\alpha \beta^2 T}{2\sigma^2} \right). \quad (1)$$

We describe each quantum model below, standardizing their structure into: (1) classical-to-quantum encoding, (2) VQC processing, and (3) measurement and decoding.

A. Quantum Attention Self-Attention (QASA)

QASA [6] implements self-attention via VQCs, the model as shown in Fig. 2. Given input sequence $\mathbf{X} \in \mathbb{R}^{T \times d}$, we compute quantum query, key, and value embeddings:

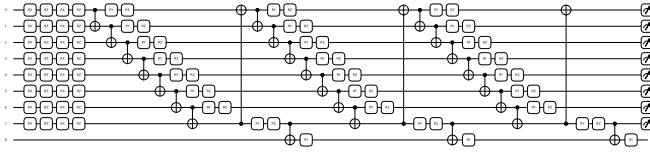


Fig. 3. The VQC used in QASA.

$$\mathbf{Q}_t = \text{VQC}_q(\mathbf{x}_t), \quad \mathbf{K}_t = \text{VQC}_k(\mathbf{x}_t), \quad \mathbf{V}_t = \text{VQC}_v(\mathbf{x}_t). \quad (2)$$

Each $\text{VQC}(\cdot)$ encodes the vector \mathbf{x}_t into quantum amplitudes, applies a variational quantum circuit composed of L layers of $RY(\theta)$ rotations and entangling CNOT gates, and measures expectation values $\langle Z_i \rangle$ on n qubits like Fig. 3.:

$$\text{VQC}(\mathbf{x}) = (\langle Z_1 \rangle, \langle Z_2 \rangle, \dots, \langle Z_n \rangle). \quad (3)$$

Each token vector $\mathbf{x}_t \in \mathbb{R}^d$ is embedded and encoded as an amplitude-encoded quantum state:

$$|\psi_t\rangle = \frac{1}{\|\mathbf{x}_t\|} \sum_{i=1}^d x_{t,i} |i\rangle. \quad (4)$$

Then a variational quantum circuit $U(\theta)$ is applied:

$$U(\theta) = \prod_{\ell=1}^L \left[\bigotimes_{i=1}^n RY(\theta_{\ell,i}) \cdot \text{CNOT}_{i,i+1} \right], \quad (5)$$

where L is the number of layers and $n = \lceil \log_2 d \rceil$ qubits are used. The output \mathbf{z}_t is obtained by measuring the expectation values of Pauli-Z operators:

$$\mathbf{z}_t = (\langle Z_1 \rangle, \dots, \langle Z_n \rangle). \quad (6)$$

Attention [16] is computed as:

$$\text{Attention}(\mathbf{Q}, \mathbf{K}, \mathbf{V}) = \text{softmax} \left(\frac{\mathbf{Q}\mathbf{K}^\top}{\sqrt{d}} \right) \mathbf{V}. \quad (7)$$

The attention output is decoded through a classical feedforward network to predict \hat{y}_{t+1} .

B. Quantum Receptance Weighted Key-Value (QRWKV)

QRWKV [5] integrates quantum evolution with the receptance attention-free model [17], the model detail is in the Fig. 4. At each time step t , the input \mathbf{x}_t is first passed through a Variational Quantum Circuit (VQC) to produce a quantum embedding:

$$\mathbf{h}_t = \text{VQC}_q(\mathbf{x}_t), \quad [\mathbf{q}_t, \mathbf{k}_t, \mathbf{v}_t] \subseteq \mathbf{h}_t. \quad (8)$$

Concretely, we prepare $|0\rangle^{\otimes n}$ and apply a parameterized circuit $U_\Theta = \prod_{\ell=1}^L U^{(\ell)}$ where

$$U^{(\ell)} = \left(\prod_{i=1}^n RY(\theta_i^{(\ell)}) \text{RZ}(\phi_i^{(\ell)}) \right) \text{EntangleLayer}, \quad (9)$$

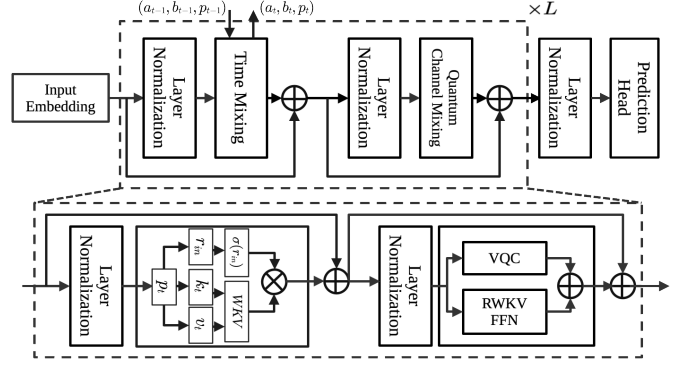


Fig. 4. Quantum RWKV architecture.

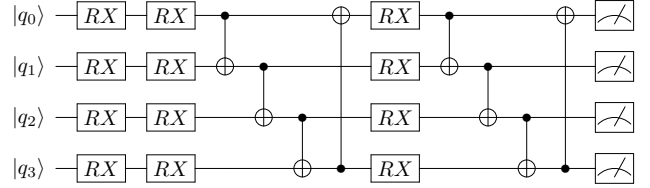


Fig. 5. The VQC used in Quantum RWKV.

and EntangleLayer applies CNOT gates in a chosen pattern. Measurement yields the vector \mathbf{h}_t , from which we split out query \mathbf{q}_t , key \mathbf{k}_t , and value \mathbf{v}_t sub-vectors.

a) *Time-Mixing and Receptance Gate*: Classical time-mixing follows the RWKV design. Project the same input \mathbf{x}_t to key and value signals:

$$\mathbf{u}_t = W^K \mathbf{x}_t, \quad \mathbf{v}_t = W^V \mathbf{x}_t, \quad (10)$$

and accumulate with exponential decay:

$$\mathbf{m}_t = \lambda \mathbf{m}_{t-1} + \mathbf{v}_t, \quad \lambda = \exp(-\Delta t/\tau). \quad (11)$$

A receptance gate controls the exposed memory:

$$\mathbf{r}_t = \sigma(W^R[\mathbf{x}_t; \mathbf{m}_{t-1}] + \mathbf{b}^R), \quad W^R \in \mathbb{R}^{d \times 2d}. \quad (12)$$

The time-mixed output is then

$$\hat{\mathbf{y}}_t^{\text{time}} = \mathbf{r}_t \odot (\mathbf{u}_t \odot \mathbf{m}_t). \quad (13)$$

b) *VQC-Enhanced Channel-Mixing*: Instead of the classical MLP input, we feed \mathbf{x}_t into the same VQC to get $\mathbf{qemb}_t = \mathbf{h}_t$, the VQC detail is in Fig. 5. The channel-mixing block becomes:

$$\mathbf{z}_t = W^1 \mathbf{qemb}_t + W^2 \text{MLP} + \mathbf{b}^1, \quad (14)$$

$$\mathbf{h}'_t = \text{GELU}(\mathbf{z}_t), \quad (15)$$

$$\mathbf{c}_t = W^3(\mathbf{h}'_t \odot \mathbf{h}'_{t-1}) + \mathbf{b}^2, \quad (16)$$

with $W^1, W^2, W^3 \in \mathbb{R}^{d \times d}$ and biases in \mathbb{R}^d . Optionally add residual connections and LayerNorm.

c) *Attention over Quantum Queries and Keys*: We also compute a measurement-based attention score between quantum-derived queries and keys:

$$\alpha_{t,\tau} = \frac{\exp\langle \mathbf{q}_t, \mathbf{k}_\tau \rangle}{\sum_{\tau'=1}^t \exp\langle \mathbf{q}_t, \mathbf{k}_{\tau'} \rangle}, \quad (17)$$

and form the attention output

$$\hat{\mathbf{y}}_{t+1}^{\text{attn}} = \sum_{\tau=1}^t \alpha_{t,\tau} \mathbf{v}_\tau. \quad (18)$$

d) *Full Layer Update*: Each layer concatenates time-mixing and VQC-enhanced channel-mixing with residuals and normalization:

$$\begin{aligned} \mathbf{h}_t &= \text{LayerNorm}(\mathbf{x}_t + \hat{\mathbf{y}}_t^{\text{time}}), \\ \mathbf{y}_t &= \text{LayerNorm}(\mathbf{h}_t + \mathbf{c}_t + \hat{\mathbf{y}}_t^{\text{attn}}). \end{aligned} \quad (19)$$

C. Quantum Long Short-Term Memory (QLSTM)

QLSTM [4] adapts classical LSTM [18] by replacing the classical neural network in each gate with a quantum neural network. A further improved version of QLSTM called linear-enhanced QLSTM [19] includes a classical neural network to preprocess the inputs before sending into QNNs. Such modifications have been shown to enhance the learning ability of QLSTM models [19]. We adopt this improvement in this benchmark as illustrated in Fig.6. Given input \mathbf{x}_t and hidden state \mathbf{h}_{t-1} , each gate is computed as:

$$\mathbf{f}_t = \sigma(\text{QNN}_f(\text{NN}_f([\mathbf{x}_t; \mathbf{h}_{t-1}])), \quad (20)$$

$$\mathbf{i}_t = \sigma(\text{QNN}_i(\text{NN}_i([\mathbf{x}_t; \mathbf{h}_{t-1}])), \quad (21)$$

$$\mathbf{o}_t = \sigma(\text{QNN}_o(\text{NN}_o([\mathbf{x}_t; \mathbf{h}_{t-1}])), \quad (22)$$

$$\mathbf{g}_t = \tanh(\text{QNN}_g(\text{NN}_g([\mathbf{x}_t; \mathbf{h}_{t-1}])). \quad (23)$$

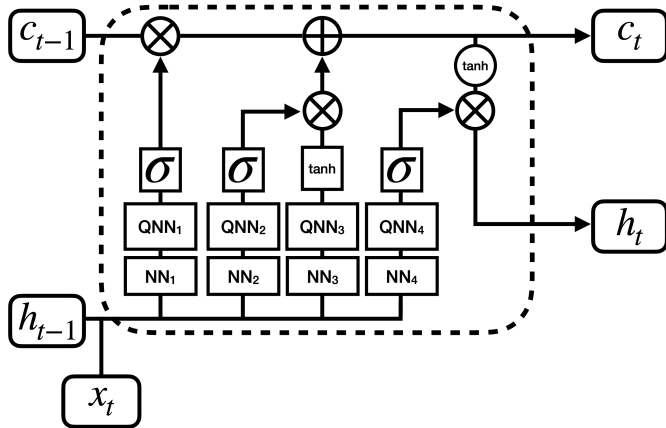


Fig. 6. Quantum LSTM architecture.

Each LSTM gate (forget, input, output, candidate) uses a separate QNN module that maps the processed classical features to quantum outputs:

$$\mathbf{f}_t = \text{QNN}_{\theta_f}(\text{NN}_{\omega_f}([\mathbf{x}_t; \mathbf{h}_{t-1}])), \quad (24)$$

where θ_f represents the trainable parameters (rotation angles) of QNN and ω_f represents the trainable weights in that particular pre-processing NN. Each gate QNN uses n qubits, initialized in $|0\rangle^{\otimes n}$, with input encoded via angle encoding:

$$U_{\text{enc}}(\mathbf{x}) = \bigotimes_{i=1}^n \text{RZ}(\arctan(x_i^2)) \text{RY}(\arctan(x_i)) \text{H}, \quad (25)$$

where the Hadamard gate H is used to create unbiased initial state,

$$(H|0\rangle)^{\otimes n} = \sum_{(q_1, q_2, \dots, q_n) \in \{0,1\}^n} \frac{1}{\sqrt{2^n}} |q_1\rangle \otimes |q_2\rangle \otimes \dots \otimes |q_n\rangle. \quad (26)$$

The encoded quantum state then goes through the trainable or variational circuit component, which includes multiple RY gates and CNOT gates. This trainable circuit block is illustrated in the dashed-line box of Fig.7. In this paper, we repeat the box 5 times so that there are $11 \times 5 = 55$ trainable parameters in each QNN. Gate values are obtained from expectation values of the Z operator (here we measure first 4 qubits to construct the hidden state). The cell state \mathbf{c}_t and hidden state \mathbf{h}_t follow standard LSTM rules. Cell state and hidden state are updated as:

$$\mathbf{c}_t = \mathbf{f}_t \odot \mathbf{c}_{t-1} + \mathbf{i}_t \odot \mathbf{g}_t, \quad \mathbf{h}_t = \mathbf{o}_t \odot \tanh(\mathbf{c}_t). \quad (27)$$

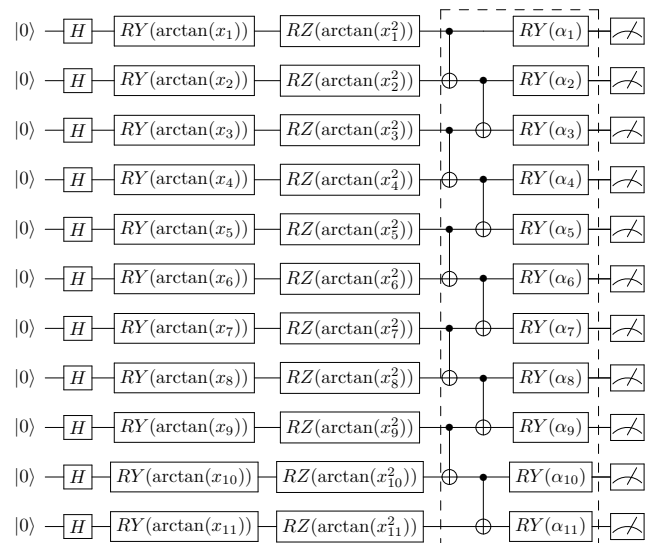


Fig. 7. Generic VQC architecture for QLSTM.

IV. EXPERIMENTS

A. Dataset and Setup

We evaluate our models on the ETTh1 dataset [7], a benchmark multivariate time series dataset from the ETT family, containing hourly data of electricity transformer

temperatures with 7 input features. We follow the common forecasting setting: given a past sequence of 16 time steps, the model predicts the next single time step.

All models are trained using the same hyperparameters: 30 epochs, batch size 64, sequence length 16, and Adam optimizer with learning rate 10^{-3} . For differential privacy training, we adopt Gaussian noise injection with ℓ_2 clipping norm of 1.0 and vary the noise multiplier $\sigma \in \{0.5, 1.0, 2.0\}$. We repeat each training setup with and without DP enabled.

B. Models and Configurations

We compare the following models:

- **Baseline (LSTM):** A standard stacked LSTM with 2 layers and hidden size 64.
- **QRWKV:** Our quantum receptance weighted key-value model with 4-qubits.
- **QASA:** The quantum variational self-attention model with 9-qubits.
- **QLSTM:** Quantum-enhanced version of LSTM integrating classical neural networks with quantum neural networks (QNNs). Each QNN operates on 11 qubits. At each time step, the concatenated vector $[\mathbf{x}_t; \mathbf{h}_{t-1}] \in \mathbb{R}^{11}$ is passed through a linear layer with input and output dimensions both equal to 11 (i.e., `nn.Linear(11, 11)`). The resulting transformed vector is then fed into the QNN for quantum processing.

Each quantum model is trained in both private and non-private settings. Experiments were conducted using simulated quantum backends, as specified in Section III.

V. RESULTS

A. Forecasting Accuracy Under Privacy Constraints

Table I reports the MAE, MSE, and RMSE of each model on the ETTh1 dataset under different noise multipliers.

B. Analysis

From the results, we observe that all models exhibit a degradation in performance as the noise multiplier increases, which is expected under stronger privacy budgets. Notably, the quantum models (QRWKV and QASA) maintain lower error metrics compared to the classical LSTM baseline across all DP settings. In particular, QASA demonstrates the best MAE and RMSE in both private and non-private regimes, highlighting its robustness to noise perturbation due to the expressiveness of quantum self-attention. This findings on multivariate dataset are the same as [20]. The QLSTM model maintains similar performance while using a much smaller model size (number of trainable parameters).

These results support our central hypothesis: *variational quantum models can preserve competitive accuracy under strict privacy constraints*, making them suitable for regulated domains such as healthcare and energy analytics.

TABLE I
FORECASTING PERFORMANCE ON ETTH1 (SEQ_LEN=16,
PRED_LEN=1)

Model	MAE	MSE	RMSE
<i>Baseline (LSTM)</i>			
No DP	0.2539	0.1208	0.3476
DP ($\sigma=0.5$)	0.2905	0.2238	0.4730
DP ($\sigma=1.0$)	0.3081	0.2389	0.4887
DP ($\sigma=2.0$)	0.3370	0.2693	0.5189
<i>QRWKV</i>			
No DP	0.2600	0.1101	0.3317
DP ($\sigma=0.5$)	0.2694	0.1212	0.3481
DP ($\sigma=1.0$)	0.2987	0.1753	0.4187
DP ($\sigma=2.0$)	0.3192	0.1980	0.4448
<i>QASA</i>			
No DP	0.2415	0.1065	0.3263
DP ($\sigma=0.5$)	0.2603	0.1324	0.3639
DP ($\sigma=1.0$)	0.2809	0.1461	0.3824
DP ($\sigma=2.0$)	0.3037	0.1766	0.4201
<i>QLSTM</i>			
No DP	0.3065	0.1618	0.4022
DP ($\sigma=0.5$)	0.2971	0.4709	0.6862
DP ($\sigma=1.0$)	0.3009	0.4045	0.6360
DP ($\sigma=2.0$)	0.3233	0.2433	0.4933

VI. CONCLUSION

We have introduced Q-DPTS, the first framework for differentially private time series forecasting using variational quantum circuits. Our method integrates classical DP-SGD with hybrid quantum models, allowing for privacy-preserving learning without sacrificing predictive accuracy. Through extensive experiments on the ETTh1 dataset, we evaluated the performance of four models under varying privacy budgets, included baseline LSTM, QRWKV, QLSTM, and QASA. The results demonstrate that quantum models, particularly QASA and QRWKV, maintain strong forecasting performance even with high noise multipliers, outperforming classical baselines in both accuracy and robustness.

Our work highlights the feasibility and effectiveness of bringing together differential privacy and quantum machine learning, opening new directions for deploying QML models in sensitive application domains.

VII. LIMITATIONS AND FUTURE WORK

Despite promising results, this work presents several limitations that warrant further exploration:

- **Quantum Simulation Only:** All experiments were performed using noiseless quantum simulators. Future studies should evaluate Q-DPTS on real quantum hardware, where gate noise and qubit decoherence may impact performance and privacy guarantees.
- **Scalability Constraints:** The current implementations are limited qubit circuits due to simulation overhead. Scaling to larger models will require architectural optimization and circuit compression.
- **Privacy Accounting:** Although we use Rényi Differential Privacy (RDP) for budget tracking, future

work should investigate tighter accounting methods or quantum-native privacy frameworks that consider quantum information-theoretic leakage.

- **Limited Forecasting Horizon:** We forecast only a single time step ahead. Extending the models to multi-step forecasting and irregular time series would improve practical applicability.
- **Application Diversity:** The evaluation is confined to the ETTh1 dataset. Broader benchmarking on financial, biomedical, or human behavioral datasets is essential to validate generalizability.

In future work, we also aim to explore quantum federated learning under DP, employ adaptive noise scheduling for utility preservation, and integrate quantum generative models for time series imputation and simulation.

REFERENCES

- [1] C. Dwork, “Differential privacy,” in *International colloquium on automata, languages, and programming*, pp. 1–12, Springer, 2006.
- [2] K. Mitarai, M. Negoro, M. Kitagawa, and K. Fujii, “Quantum circuit learning,” *Physical Review A*, vol. 98, no. 3, p. 032309, 2018.
- [3] I. Mironov, “Rényi differential privacy,” in *2017 IEEE 30th computer security foundations symposium (CSF)*, pp. 263–275, IEEE, 2017.
- [4] S. Y.-C. Chen, S. Yoo, and Y.-L. L. Fang, “Quantum long short-term memory,” in *ICASSP 2022-2022 IEEE International Conference on Acoustics, Speech and Signal Processing (ICASSP)*, pp. 8622–8626, IEEE, 2022.
- [5] C.-S. Chen and E.-J. Kuo, “Quantum-enhanced channel mixing in rwkv models for time series forecasting,” *arXiv preprint arXiv:2505.13524*, 2025.
- [6] C.-S. Chen and E.-J. Kuo, “Quantum adaptive self-attention for quantum transformer models,” *arXiv preprint arXiv:2504.05336*, 2025.
- [7] H. Zhou, S. Zhang, J. Peng, S. Zhang, J. Li, H. Xiong, and W. Zhang, “Informer: Beyond efficient transformer for long sequence time-series forecasting,” in *Proceedings of the AAAI conference on artificial intelligence*, vol. 35, pp. 11106–11115, 2021.
- [8] J. Biamonte, P. Wittek, N. Pancotti, P. Rebentrost, N. Wiebe, and S. Lloyd, “Quantum machine learning,” *Nature*, vol. 549, pp. 195–202, 2017.
- [9] S. Z. Khan, N. Muzammil, S. Ghafoor, H. Khan, S. M. H. Zaidi, A. J. Aljohani, and I. Aziz, “Quantum long short-term memory (qlstm) vs. classical lstm in time series forecasting: a comparative study in solar power forecasting,” *Frontiers in Physics*, vol. 12, p. 1439180, 2024.
- [10] N. Liu and P. Rebentrost, “Quantum machine learning for quantum anomaly detection,” *Physical Review A*, vol. 97, no. 4, p. 042315, 2018.
- [11] J. Du, S. Li, X. Chen, S. Chen, and M. Hong, “Dynamic differential-privacy preserving sgd,” *arXiv preprint arXiv:2111.00173*, 2021.
- [12] H. B. McMahan, D. Ramage, K. Talwar, and L. Zhang, “Learning differentially private recurrent language models,” *arXiv preprint arXiv:1710.06963*, 2017.
- [13] Z. Yang, B. Xiong, K. Chen, L. T. Yang, X. Deng, C. Zhu, and Y. He, “Differentially private federated tensor completion for cloud–edge collaborative aiot data prediction,” *IEEE Internet of Things Journal*, vol. 11, no. 1, pp. 256–267, 2023.
- [14] L. Zhou and M. Ying, “Differential privacy in quantum computation,” in *2017 IEEE 30th Computer Security Foundations Symposium (CSF)*, pp. 249–262, IEEE, 2017.
- [15] W. M. Watkins, S. Y.-C. Chen, and S. Yoo, “Quantum machine learning with differential privacy,” *Scientific Reports*, vol. 13, no. 1, p. 2453, 2023.
- [16] A. Vaswani, N. Shazeer, N. Parmar, J. Uszkoreit, L. Jones, A. N. Gomez, L. Kaiser, and I. Polosukhin, “Attention is all you need,” *Advances in neural information processing systems*, vol. 30, 2017.
- [17] B. Peng, E. Alcaide, Q. Anthony, A. Albalak, S. Arcadinho, H. Cao, X. Cheng, M. Chung, M. Greiner, L. GV, *et al.*, “Rwkv: Reinventing rnns for the transformer era,” *Findings of the Association for Computational Linguistics: EMNLP 2023*, pp. 14048–14077, 2023.
- [18] S. Hochreiter and J. Schmidhuber, “Long short-term memory,” *Neural Computation*, vol. 9, no. 8, pp. 1735–1780, 1997.
- [19] Y. Cao, X. Zhou, X. Fei, H. Zhao, W. Liu, and J. Zhao, “Linear-layer-enhanced quantum long short-term memory for carbon price forecasting,” *Quantum Machine Intelligence*, vol. 5, no. 2, p. 26, 2023.
- [20] C.-S. Chen, X. Zhang, and Y.-C. Chen, “Quantum reinforcement learning trading agent for sector rotation in the taiwan stock market,” *arXiv preprint arXiv:2506.20930*, 2025.